

Ferrocenyl-Substituted Metallacycles of Titanocenes: Oligocyclopentadienyl Complexes with Promising Properties**

Katharina Kaleta, Alexander Hildebrandt, Frank Strehler, Perdita Arndt, Haijun Jiao, Anke Spannenberg, Heinrich Lang,* and Uwe Rosenthal*

Dedicated to Professor Gerhard Erker in occasion of his 65th birthday

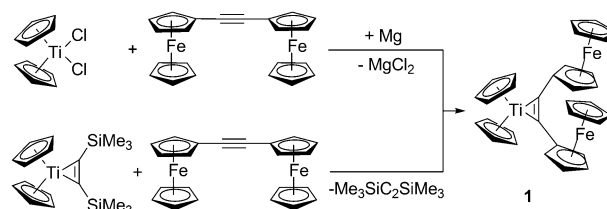
Not only the diverse functionalities but also the aesthetic pleasures of highly symmetrical molecules fascinate chemists. In 1952, Eiland and Pepinsky reported the molecular structure of ferrocene in the solid state ($[\text{Cp}_2\text{Fe}]$, $\text{Cp} = \eta^5\text{-C}_5\text{H}_5$) which represents the first example of an attractive sandwich molecule.^[1] To date, numerous metallocene complexes have been synthesized and found wide application.^[2] In 2006, Vollhardt and co-workers reported the syntheses and molecular structures of hexaferrocenylbenzene (C_6Fc_6 , $\text{Fc} = (\eta^5\text{-C}_5\text{H}_4\text{Fc})\text{Cp}$)^[3] and the penta(ferrocenyl)cyclopentadienyl tricarbonyl manganese complex $[(\eta^5\text{-C}_5\text{Fc}_5)\text{Mn}(\text{CO})_3]$.^[4] They emphasized the great interest of these molecules with potential applications in electronics, optics, and catalysis. Similar attractive molecular structures are found in compounds like hexakis(4-ferrocenylphenyl)benzene ($\text{C}_6(\text{C}_6\text{H}_4\text{Fc})_6$), hexakis(ferrocenylethynyl)benzene ($\text{C}_6(\text{C}\equiv\text{C}\text{Fc})_6$, $\text{Fc}' = \text{substituted ferrocenyl}$) and $[(\text{FcCp})_3(\text{trindenyl})]$.^[5] In 2011, super-crowded ferrocenyl-substituted five-membered heterocycles ($\text{C}_4\text{Fc}_4\text{X}$, $\text{X} = \text{O}, \text{S}, \text{NR}$) were added to this family of compounds.^[6] Their interesting electronic properties were studied in detail by spectroelectrochemistry.

Our interest in small and highly strained metallacycles of Group 4 metallocenes led us to consider the accessibility and stability of analogous ferrocenyl-substituted complexes with novel electrochemical properties.^[7] The smallest example is the metallacyclopentadiene complex formed formally by alkyne addition to a metal center.^[8] To date, the structures of several monoferrocenyl-substituted acetylenes coordinated to different metal carbonyls have been described.^[9] In 1967, King and co-workers reported a diferrocenylacetylene cobalt carbonyl complex,^[10] but its molecular structure was not verified by X-ray analysis. Mach and co-workers synthesized and charac-

terized titanocene complexes with the monoferrocenyl-substituted alkynes $\text{FcC}\equiv\text{CR}$ ($\text{R} = \text{SiMe}_3, \text{Ph}$).^[11]

We report herein on the synthesis and structural and electrochemical properties of complexes **1** and **2** which were obtained by addition of diferrocenylacetylene ($\text{FcC}\equiv\text{CFC}$)^[12] and 1,4-diferrocenylbuta-1,3-diyne ($\text{FcC}\equiv\text{CC}\equiv\text{CFC}$)^[13] to titanocene complexes. Their physical and chemical properties are studied and discussed in detail along with density functional theory computations.

Scheme 1 shows the synthesis of complex **1**, which was obtained either by reduction of $[\text{Cp}_2\text{TiCl}_2]$ with Mg in the presence of $\text{FcC}\equiv\text{CFC}$ or by alkyne exchange of $[\text{Cp}_2\text{Ti}(\eta^2\text{-Me}_3\text{SiC}_2\text{SiMe}_3)]$ ^[14] in a slower reaction. Recrystallization from toluene at -78°C gave brown single crystals of **1** suitable for X-ray crystal structure analysis (Figure 1). The central carbon atoms C1 and C2 of the coordinated alkyne form a titanacyclopentadiene. Both ferrocenyl groups point parallel in the same direction, resulting in a symmetric arrangement out of three metallocene fragments. The long



Scheme 1. Synthesis of ferrocenyl-substituted titanacyclopentadiene **1**.

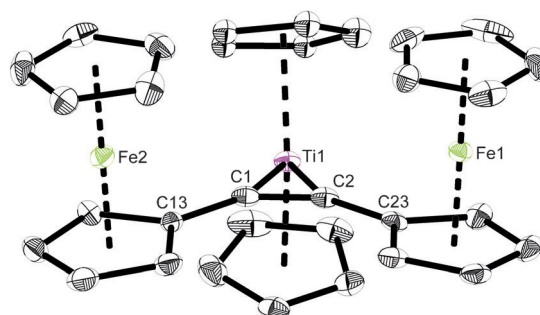


Figure 1. Molecular structure of **1**. Hydrogen atoms are omitted for clarity. The thermal ellipsoids correspond to 30% probability. Selected bond lengths [Å] and angles [°]: C1–C2 1.288(8), C1–C13 1.460(7), C2–C23 1.446(7), Ti1–C1 2.076(5), Ti1–C2 2.088(5); C1–Ti1–C2 36.0(2) Ti1–C1–C13 142.2(4), Ti1–C2–C23 144.4(4).

[*] K. Kaleta, Dr. P. Arndt, Dr. H. Jiao, Dr. A. Spannenberg, Prof. Dr. U. Rosenthal
Leibniz-Institut für Katalyse e.V. an der Universität Rostock
Albert-Einstein-Strasse 29a, 18059 Rostock (Germany)
E-mail: uwe.rosenthal@catalysis.de

A. Hildebrandt, F. Strehler, Prof. Dr. H. Lang
Technische Universität Chemnitz
Lehrstuhl für Anorganische Chemie
Strasse der Nationen 62, 09111 Chemnitz (Germany)
E-mail: heinrich.lang@chemie.tu-chemnitz.de

[**] Support by the Deutsche Forschungsgemeinschaft (RO 1269/8-1) and the Fonds der chemischen Industrie is acknowledged.

Supporting information for this article is available on the WWW under <http://dx.doi.org/10.1002/anie.201105248>.

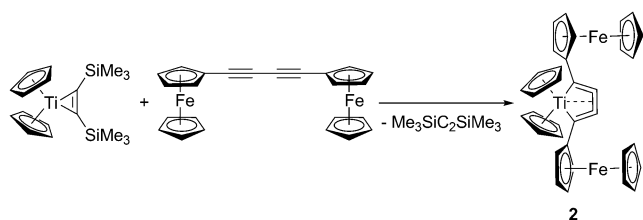
Ti–Fe distances of 4.9 Å exclude direct intermetallic interaction.

The central C1–C2 bond of 1.288(8) Å is in the range of typical C=C bonds in cyclopropenes.^[15] The ferrocenyl groups shorten the Ti–C distances, as can be seen by the comparison of **1** ($d(\text{Ti}–\text{C}) = 2.076(5), 2.088(5)$ Å) with $[\text{Cp}'_2\text{Ti}(\eta^2\text{-FcC}_2\text{SiMe}_3)]$ (2.073(2) (Fc), 2.115(2) (SiMe₃); Cp' = $\eta^5\text{-C}_5\text{Me}_4\text{H}$)^[11] and $[\text{Cp}_2\text{Ti}(\eta^2\text{-Me}_3\text{SiC}_2\text{SiMe}_3)]$ (2.136(5), 2.139(4))^[16] which indicates a stronger coordination of the alkyne to **1**.

In the $^{13}\text{C}\{^1\text{H}\}$ NMR spectrum the central atoms C1 and C2 in **1** are magnetically equivalent and are observed at $\delta_{\text{C}} = 191.8$ ppm. The ferrocenyl groups show three ^{13}C signals ($\delta_{\text{C}} = 68.1, 69.2, 86.3$ ppm), whereas the signal of the rotating C₅H₅ groups falls together with the CH groups in the C₅H₄ moiety, thus indicating a free rotation of the C–Fc bonds in solution. Compared to $[\text{Cp}'_2\text{Ti}(\eta^2\text{-FcC}_2\text{SiMe}_3)]$ ($\delta_{\text{C}} = 210.9, 217.8$ ppm)^[11] and $[\text{Cp}_2\text{Ti}(\eta^2\text{-Me}_3\text{SiC}_2\text{SiMe}_3)]$ ($\delta_{\text{C}} = 244.7$ ppm),^[14] the $^{13}\text{C}\{^1\text{H}\}$ NMR signal in **1** is strongly shifted to higher fields owing to the exchange of the SiMe₃ substituent by ferrocenyl groups.

Encouraged by the availability of complex **1**, we were interested in the synthesis of a Fc-substituted titanacyclopenta-2,3,4-triene (**2**), which would result in an enlargement of the conjugated system. To the best of our knowledge such Fc-substituted cumulenes have not been structurally characterized to date, but complexes in which 1,4-diferrocenylbuta-1,3-diene coordinates to M₂(CO)₆ (M = Fe, Ru), W(CO)₃ (forming a dimer), or RuCpBr are known.^[17] Furthermore, complexes of FcC≡CC≡CFc with trinuclear metal carbonyls (M = Co, Ru, Os) were reported, but small metallacycles were not formed in this case.^[18]

The alkyne exchange reaction of $[\text{Cp}_2\text{Ti}(\eta^2\text{-Me}_3\text{SiC}_2\text{SiMe}_3)]$ with FcC≡CC≡CFc in toluene resulted in the formation of metallacycle **2** (Scheme 2). Recrystallization from toluene at ambient temperature gave red single crystals of **2** suitable for X-ray structure analysis (Figure 2). The titanium atom forms a planar five-membered ring with the four central carbon atoms of the ligand. Unlike in **1**, the ferrocenyl substituents in **2** are oriented antiparallel on opposite sides. The central C2–C3 bond corresponds to a C=C bond,^[15] whereas the adjacent C1–C2 and C3–C4 bonds are shorter but are still in the range of a double bond. Thus, the central ring can be best described as a metallacyclocumulene with three connected C=C bonds.^[19] All four Ti–C distances are typical for single bonds (cf. 2.213(2) Å in $(\eta^5\text{-C}_5\text{Me}_4\text{SiMe}_3)_2\text{TiMe}$)^[20]. The important bond lengths and angles are not significantly different than in $[\text{Cp}_2\text{Ti}(\eta^4\text{-tBuC}_4\text{tBu})]$.^[19]



Scheme 2. Synthesis of complex **2**.

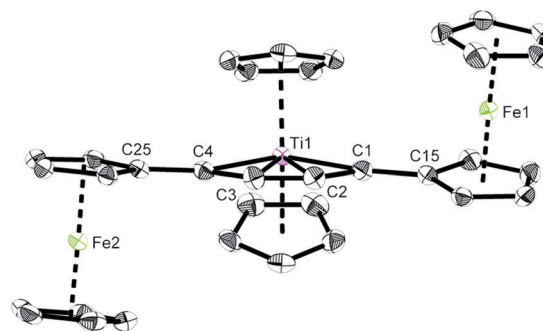


Figure 2. Molecular structure of **2**. Hydrogen atoms are omitted for clarity. The thermal ellipsoids correspond to 50% probability. Selected bond lengths [Å] and angles [°]: C1–C2 1.283(2), C2–C3 1.326(2), C3–C4 1.282(2), C1–C15 1.435(2), C4–C25 1.435(2), Ti1–C1 2.230(2), Ti1–C2 2.218(2), Ti1–C3 2.213(2), Ti1–C4 2.249(2); C1–Ti1–C4 101.74(6), C1–C2–C3 146.1(2), C2–C3–C4 147.6(2), Ti1–C1–C15 146.60(11), Ti1–C4–C25 147.02(12).

One singlet in the ^1H NMR spectrum of the titanocene Cp rings ($\delta_{\text{H}} = 5.20$ ppm) and two signals in the $^{13}\text{C}\{^1\text{H}\}$ NMR spectrum for the quaternary carbon atoms in the metallacycle ($\delta_{\text{C}} = 97.7$ and 169.7 ppm) indicate a symmetric structure. The four ^{13}C signals of the Fc groups ($\delta = 70.1, 70.2, 72.7, 81.1$ ppm) in solution reveal free rotation of the C–Fc bond as in complex **1**.

The calculated minimum-energy structures of **1** and **2** have C_s and C₂ symmetry, respectively, and their optimized structural parameters agree very well with those from X-ray structure analysis (see the Supporting Information). The *trans* form of **1** is slightly more stable than the *cis* form ($\Delta G = -2.05$ kcal mol^{−1}), while both *trans* and *cis* forms of **2** are nearly isoenergetic ($\Delta G = -0.02$ kcal mol^{−1}). These small energy differences support the results from the $^{13}\text{C}\{^1\text{H}\}$ NMR spectroscopy measurements, which reveal a structural flexibility of **1** and **2** in solution. Therefore, the different orientation in the solid state might be explained by packing effects.

The redox properties of **1** and **2** were studied by cyclic voltammetry utilizing 0.1 M $[\text{NBu}_4][\text{B}(\text{C}_6\text{F}_5)_4]$ in dry THF as supporting electrolyte. The results carried out at a scan rate of 100 mV s^{−1} are shown in Figure 3 and Table 1. All potentials are referenced to the FcH/FcH⁺ redox couple as recommended by IUPAC.^[21] Complexes $[\text{Cp}_2\text{Ti}(\eta^2\text{-Me}_3\text{SiC}_2\text{SiMe}_3)]$ and $[\text{Cp}_2\text{Ti}(\eta^4\text{-tBuC}_4\text{tBu})]$ were measured as non-Fc-containing analogues for which only one irreversible metallacycle-based oxidation could be detected. The potential of this process seems to be highly dependent on the nature of the substituents and on the geometry of the complex itself. Complexes **1** and **2** could be oxidized in three consecutive redox processes. The differences between the oxidations and respective reduction events (ΔE_{p}) for the redox processes in **2** are in the range between 61 and 90 mV, confirming their reversibility, while those of **1** possess ΔE_{p} values of 110 to 140 mV. Furthermore, multicyclic experiments revealed that **1** decomposes during the measurement and deposits at the electrode. The irreversibility of the redox processes of **1** and especially the broad wave of the third oxidation step leads to

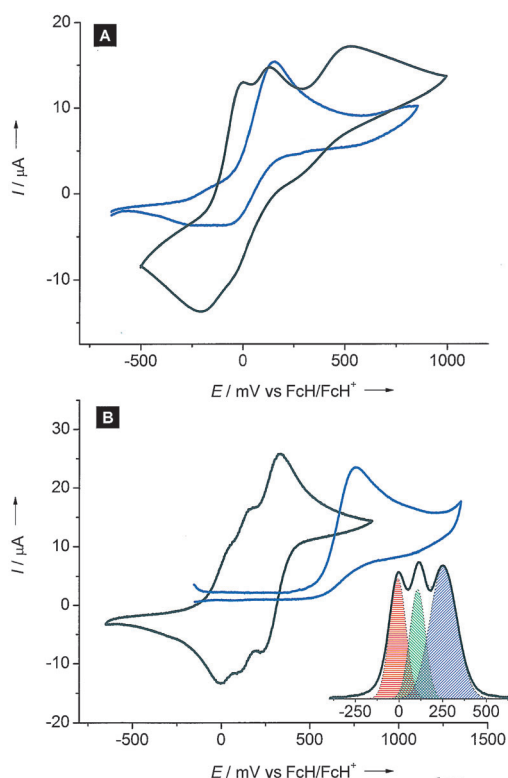


Figure 3. Cyclic voltammograms at 25 °C; supporting electrolyte: 0.1 mol L⁻¹ [NBu₄][B(C₆F₅)₄] in dry THF: A) molecule **1** (black) and [Cp₂Ti(η²-Me₃SiC₂SiMe₃)] (blue) for comparison; B) molecule **2** (black) and [Cp₂Ti(η⁴-tBuC₄tBu)] (blue) for comparison. Inset: the square-wave voltammogram of **2**; the different peak areas reveal a 1:1:2 ratio.

Table 1: Electrochemical data of **1**, **2**, and [Cp₂Ti(η²-Me₃SiC₂SiMe₃)], [Cp₂Ti(η⁴-tBuC₄tBu)], FcC≡Cfc, and FcC≡CC≡Cfc for comparison.

Compound	E_1^0 [mV] (ΔE_p [mV])	E_2^0 [mV] (ΔE_p [mV])	E_3^0 [mV] (ΔE_p [mV])
1			
[Cp ₂ Ti(η ² -Me ₃ SiC ₂ SiMe ₃)]	-85 (110)	40 (140)	520 ^[a]
FcC≡Cfc	150 ^[a]	—	—
2	20 (65)	265 (72)	—
[Cp ₂ Ti(η ⁴ -tBuC ₄ tBu)]	30 (71)	130 (61)	280 (90)
FcC≡CC≡Cfc	750 ^[a]	—	—
	135 (64)	291 (76)	—

[a] Irreversible oxidation.

the conclusion that **1** is unstable and decomposes, at least as the dication **1**²⁺. Calculations of the radical cations **1**^{•+} and **2**^{•+} reveal that **1**^{•+} is not stable in THF. The alkyne ligand can be replaced by THF to form [Cp₂Ti(thf)₂]^{•+} ($\Delta G = -3.20$ kcal mol⁻¹), which has been synthesized and structurally characterized.^[22] Unfortunately, complexes **1** and **2** are not stable in halogenated solvents. In contrast, **2**^{•+} and **2**²⁺ are stable in THF ($\Delta G = +6.93$ and 27.11 kcal mol⁻¹, respectively), and **2**^{•+} still retains the metallacycle structure as shown in Figure 4. Furthermore, the preparative oxidation of **2** with different ratios of [Ag(toluene)₃][B(C₆F₅)₄] (1:1 and 1:2) and AgPF₆ (1:4), respectively, did not result in the formation of FcC≡CC≡Cfc. Therefore, complex **2** is stable under oxidizing conditions, unlike complex **1**, which decomposes to FcC≡Cfc.

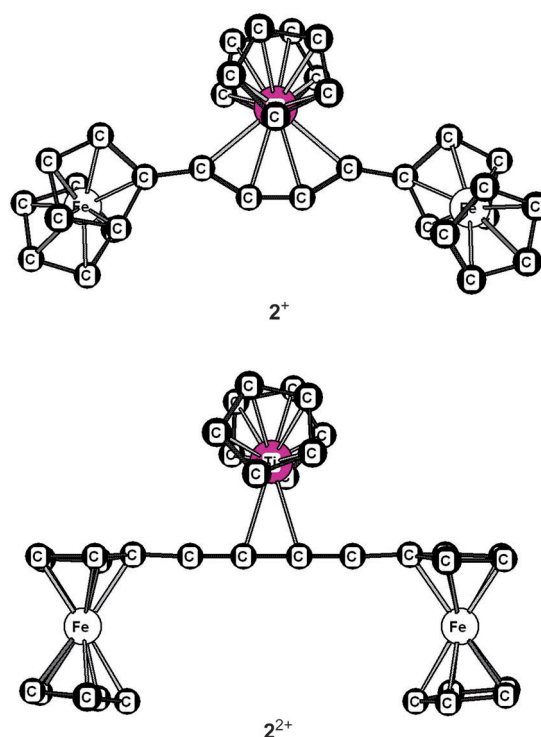


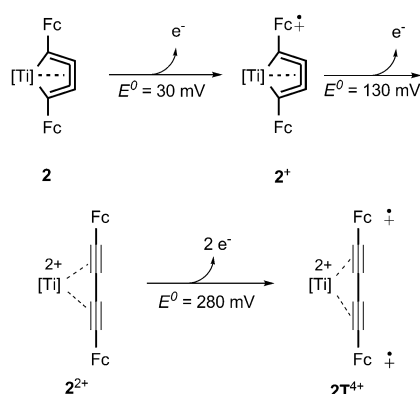
Figure 4. BP86/TZVP optimized structures of **2**^{•+} and **2**²⁺.

Unfortunately, we did not succeed in the isolation or characterization of the cationic species. Owing to the instability of complex **1** during the measurements, further investigations on the mechanism of the oxidation were limited to compound **2**.

The first two oxidation steps of complex **2** most likely take place at the ferrocenyl groups. Computations reveal strong structural changes after the second oxidation. As shown in Figure 4, the five-membered ring is destroyed and the C₄ carbon chain becomes linear. The geometry optimization of **2**²⁺ from the cyclic form results directly in the open-chain form without any barrier. Moreover, the low-lying triplet state of the dication complex is very close in energy to the singlet state ($\Delta H = 1.63$ kcal mol⁻¹ or $\Delta G = -0.51$ kcal mol⁻¹).

The third oxidation is a simultaneous two-step, one-electron redox process, as demonstrated by deconvolution of the square wave voltammetric measurements (see inset Figure 3). Computations on the tetracation **2**⁴⁺ show that the minimum-energy structure has a triplet ground state **2T**⁴⁺ with spin densities at the two iron centers (1.208), and the corresponding singlet state **2S**⁴⁺ is higher in energy by 52.86 kcal mol⁻¹. The structure of **2T**⁴⁺ resembles that of **2**²⁺. For comparison, the triplet state of the FcC≡CC≡Cfc dication is 11.37 kcal mol⁻¹ more stable than the singlet state.

These results, together with the cyclic voltammetry measurements and the natural bond orbital analysis (see natural charge and Wiberg bond index in the Supporting Information), make it possible to propose a simplified oxidation mechanism of complex **2** (Scheme 3). On the basis of the computed spin density and the natural charge on the Fe and Ti atoms, the first oxidation step takes place at the iron centers. After the second oxidation step, the five-membered



Scheme 3. Proposed mechanism for the oxidation of **2** to **2T⁴⁺**.

ring in **2²⁺** collapses spontaneously and the C₄ chain becomes linear. Furthermore, the singlet **2²⁺** can be considered as the combination of a {Cp₂Ti²⁺} fragment and FcC≡CC≡CFc with reduced triple-bond character. This structural change is supported by an observed C≡C vibration mode for **2²⁺** in the in situ IR measurements (Supporting Information Figure S2) and plausibly explains the much lower oxidation potential for **2** than for [Cp₂Ti(η⁴-tBuC₄tBu)]. In the final oxidation state **2T⁴⁺**, the spin densities, natural charge, and bond index analysis reveal a {Cp₂Ti²⁺} fragment and a ⁺FcC≡CC≡CFc⁺ chain that mimics the oxidation of FcC≡CC≡CFc into the dication (see the Supporting Information).

In situ UV/Vis/NIR measurements did not show an intervalence charge transfer (IVCT) band for **2** in any oxidation state (Supporting Information Figure S1). Therefore, the interferrocenyl interactions seem to be limited to electrostatic effects, and the mixed-valence compound is charge localized. It is therefore appropriate to classify compound **2⁺** as class I species according to Robin and Day.^[23] In contrast to the cyclic voltammetry and in situ UV/Vis/NIR results, the minimum-energy structure of **2²⁺** has C₂ symmetry, thus indicating that the unpaired electron in **2²⁺** is delocalized over the system; this situation represents a mixed-valence state. The atomic spin densities are found mainly at the two iron centers (0.420/Fe), and the spin density at the titanium center is very low (0.03). Breaking the symmetry (C₂→C₁) does not result in a more stable state. Probably a solvent effect destabilizes the mixed-valence state, as reported in the literature.^[24]

In conclusion, the reaction of in situ generated titanocene with diferrocenylacetylene and 1,4-diferrocenylbuta-1,3-diyne results in naked C₂ and C₄ units surrounded by three metallocene groups. These compounds are unique examples of diferrocenyl-substituted small ring systems that were analyzed by X-ray crystallography. The aromatic substituents allowed for the electronic interaction between different metals to be studied. (Spectro-)electrochemical measurements reveal a stepwise oxidation of the iron centers and the metallacycle, respectively. Compound **1** is not stable under oxidizing conditions. The two ferrocenyl groups in compound **2** are oxidized, whereas an electron transfer from the metallacycle to the iron centers leads to linearization of the ligand.

Interestingly, the complexation of the conjugated diferrocenyl compounds by titanocene reduces the charge delocalization between the two iron centers. Further investigations regarding the influence of the Group 4 metal on the reactivity and electrochemical properties are in progress.

Received: July 26, 2011

Published online: October 4, 2011

Keywords: density functional calculations · electrochemistry · heterometallic complexes · metallacycles · titanocenes

- [1] P. F. Eiland, R. Pepinsky, *J. Am. Chem. Soc.* **1952**, *74*, 4971–4971.
- [2] Selected examples: a) G. Gasser, I. Ott, N. Metzler-Nolte, *J. Med. Chem.* **2011**, *54*, 3–25; b) D. Astruc, C. Ornelas, J. Ruiz, *Acc. Chem. Res.* **2008**, *41*, 841–856; c) A.-S. Rodrigues, E. Kirillov, J.-F. Carpentier, *Coord. Chem. Rev.* **2008**, *252*, 2115–2136.
- [3] Y. Yu, A. D. Bond, P. W. Leonard, U. J. Lorenz, T. V. Timofeeva, K. P. C. Vollhardt, G. D. Whitener, A. A. Yakovenko, *Chem. Commun.* **2006**, 2572–2574, and references therein.
- [4] Y. Yu, A. D. Bond, P. W. Leonard, K. P. C. Vollhardt, G. D. Whitener, *Angew. Chem.* **2006**, *118*, 1826–1831; *Angew. Chem. Int. Ed.* **2006**, *45*, 1794–1799.
- [5] a) V. J. Chebny, D. Dhar, S. V. Lindeman, R. Rathore, *Org. Lett.* **2006**, *8*, 5041–5044; b) A. K. Diallo, J.-C. Daran, F. Varret, J. Ruiz, D. Astruc, *Angew. Chem.* **2009**, *121*, 3187–3191; *Angew. Chem. Int. Ed.* **2009**, *48*, 3141–3145; c) S. Santi, L. Orian, A. Donoli, A. Bisello, M. Scapinello, F. Benetollo, P. Ganis, A. Ceccon, *Angew. Chem.* **2008**, *120*, 5411–5414; *Angew. Chem. Int. Ed.* **2008**, *47*, 5331–5334.
- [6] a) A. Hildebrandt, T. Rüffer, E. Erasmus, J. C. Swarts, H. Lang, *Organometallics* **2010**, *29*, 4900–4905; b) A. Hildebrandt, D. Schaarschmidt, L. van As, J. C. Swarts, H. Lang, *Inorg. Chim. Acta* **2011**, *374*, 112–118; c) A. Hildebrandt, D. Schaarschmidt, H. Lang, *Organometallics* **2011**, *30*, 556–563; d) A. Hildebrandt, D. Schaarschmidt, R. Claus, H. Lang, *Inorg. Chem.* **2011**, DOI: 10.1021/ic200926z.
- [7] W. H. Morrison, D. N. Hendrickson, *Inorg. Chem.* **1975**, *14*, 2331–2346.
- [8] V. V. Burlakov, A. V. Polyakov, A. I. Yanovsky, Y. T. Struchkov, V. B. Shur, M. E. Vol'pin, U. Rosenthal, H. Görls, *J. Organomet. Chem.* **1994**, *476*, 197–206.
- [9] Selected examples: a) E. Delgado, E. Hernandez, A. Nieves, A. Martin, M. J. Recio, *J. Organomet. Chem.* **2010**, *695*, 446–452; b) A. D. Woods, G. Alcalde, V. B. Golovko, C. M. Halliwell, M. J. Mays, J. M. Rawson, *Organometallics* **2005**, *24*, 628–637; c) H. Schottenberger, J. Lukasser, E. Reichel, A. G. Müller, G. Steiner, H. Kopacka, K. Wurst, K. H. Ongania, K. Kirchner, *J. Organomet. Chem.* **2001**, *637*, 558–576.
- [10] M. Rosenblum, N. Brawn, B. King, *Tetrahedron Lett.* **1967**, *8*, 4421–4425.
- [11] P. Štěpnička, R. Gyepes, I. Císařová, V. Varga, M. Polášek, M. Horáček, K. Mach, *Organometallics* **1999**, *18*, 627–633.
- [12] M. Rosenblum, N. Brawn, J. Papenmeier, M. Applebaum, *J. Organomet. Chem.* **1966**, *6*, 173–180.
- [13] Z. Yuan, G. Stringer, I. R. Jobe, D. Kreller, K. Scott, L. Koch, N. J. Taylor, T. B. Marder, *J. Organomet. Chem.* **1993**, *452*, 115–120.
- [14] V. V. Burlakov, A. V. Polyakov, A. I. Yanovsky, Y. T. Struchkov, V. B. Shur, M. E. Vol'pin, U. Rosenthal, H. Görls, *J. Organomet. Chem.* **1994**, *476*, 197–206.
- [15] F. H. Allen, O. Kennard, D. G. Watson, L. Brammer, A. G. Orpen, R. Taylor, *J. Chem. Soc. Perkin Trans. 2* **1987**, S1–S19.

- [16] U. Rosenthal, V. V. Burlakov, P. Arndt, W. Baumann, A. Spannenberg, *Organometallics* **2003**, 22, 884–900.
- [17] a) P. Mathur, S. Chatterjee, A. Das, S. M. Mobin, *J. Organomet. Chem.* **2007**, 692, 819–823; b) P. Mathur, A. K. Singh, V. K. Singh, P. Singh, R. Rahul, S. M. Mobin, C. Thöne, *Organometallics* **2005**, 24, 4793–4798; c) Y. Yamada, J. Mizutani, M. Kurihara, H. Nishihara, *J. Organomet. Chem.* **2001**, 637–639, 80–83; d) A. A. Koridze, A. I. Yanovsky, Y. T. Struchkov, *J. Organomet. Chem.* **1992**, 441, 277–284.
- [18] a) M. I. Bruce, B. W. Skelton, A. H. White, N. N. Zaitseva, *J. Organomet. Chem.* **2002**, 650, 188–197; b) E. Champeil, S. M. Draper, *J. Chem. Soc. Dalton Trans.* **2001**, 1440–1447; c) R. D. Adams, B. Qu, *J. Organomet. Chem.* **2001**, 620, 303–307; d) R. D. Adams, B. Qu, *J. Organomet. Chem.* **2001**, 619, 271–274; e) R. D. Adams, B. Qu, *Organometallics* **2000**, 19, 2411–2413.
- [19] V. V. Burlakov, A. Ohff, C. Lefebvre, A. Tillack, W. Baumann, R. Kempe, U. Rosenthal, *Chem. Ber.* **1995**, 128, 967–971.
- [20] J. Pinkas, L. Lukešová, R. Gyepes, I. Cisařová, P. Lönnecke, J. Kubišta, M. Horáček, K. Mach, *Organometallics* **2007**, 26, 3100–3110.
- [21] G. Gritzner, J. Kuta, *Pure Appl. Chem.* **1984**, 56, 461–466.
- [22] a) A. Ohff, R. Kempe, W. Baumann, U. Rosenthal, *J. Organomet. Chem.* **1996**, 520, 241–244; b) W. Ahlers, B. Temme, G. Erker, R. Fröhlich, F. Zippel, *Organometallics* **1997**, 16, 1440–1444.
- [23] M. B. Robin, P. Day, *Adv. Inorg. Chem. Radiochem.* **1968**, 10, 247–423.
- [24] F. Ding, H. Wang, Q. Wu, T. van Voorhis, S. Chen, J. P. Konopelski, *J. Phys. Chem. A* **2010**, 114, 6039–6046.